Biophysical Journal, Volume *119*

Supplemental Information

Non-Langmuir Kinetics of DNA Surface Hybridization

Luka Vanjur, Thomas Carzaniga, Luca Casiraghi, Marcella Chiari, Giuliano Zanchetta, and Marco Buscaglia

1. Conversion of reflected intensity into surface density of molecules

The apparatus and the analysis algorithm of the RPI method was described in (1). Briefly, the spotted surface of the glass sensor was illuminated by collimated LED light at 450 nm and sequences of images of the reflected light were acquired by a CCD camera. The conversion of the brightness of the RPI image pixels of the spot region, u_s, and outside the spots, u_0, into surface density was performed according to:

$$\sigma(t) = \sigma^* \sqrt{\frac{u_s(t)}{u_0} - 1} - \delta\sigma \quad (1)$$

where σ^*, u_0 and $\delta\sigma$ are obtained according to (1) from the physical parameters of the RPI sensor and the refractive index of the solution.

2. Amount of hybridized DNA target strands at equilibrium

Single strand DNA oligomers with a length of 12 bases (probe type p1 in Table 1 and Figure 1) were immobilized on the surface of a RPI label-free sensor. The injection into the RPI measuring cell of complementary target ssDNA provided an increase of the measured surface density of molecules due to hybridization of the surface probes with the targets. The real-time hybridization curves were acquired from spots with different number surface density of probes s_p, after the addition of targets in solution at the concentration c_t =100 nM. The measured curves are reported in Figure 2. All curves reached a stable asymptotic value of target mass surface density σ_{eq} at long time. The asymptotic amplitude of each curve, converted from σ_{eq} into the number surface density of target at equilibrium s_{eq}, is reported in Figure S1 as a function of s_p. The number of captured target strands was roughly proportional to the number of surface probes. The hybridization yield ψ, that is the fraction of surface probes hybridized with the target, was about 30%, indicating that a fraction of probe strands on the surface were not accessible to the target.

In the framework of the NLER kinetic model described by Eq. 6, the asymptotic amplitude reached at saturation of the probe sites, i.e. at large c_t, remains proportional to the surface density of probes. However, increasing the surface density of probes, the apparent equilibrium constant for dissociation also increases (see Figure 5b), hence the saturation is reached at larger values of c_t. Accordingly, at constant c_t, the observed asymptotic amplitude deviates from a linear scaling with s_p, as shown by the dashed line in Figure S1, obtained from the numerical solutions of Eq. 6.

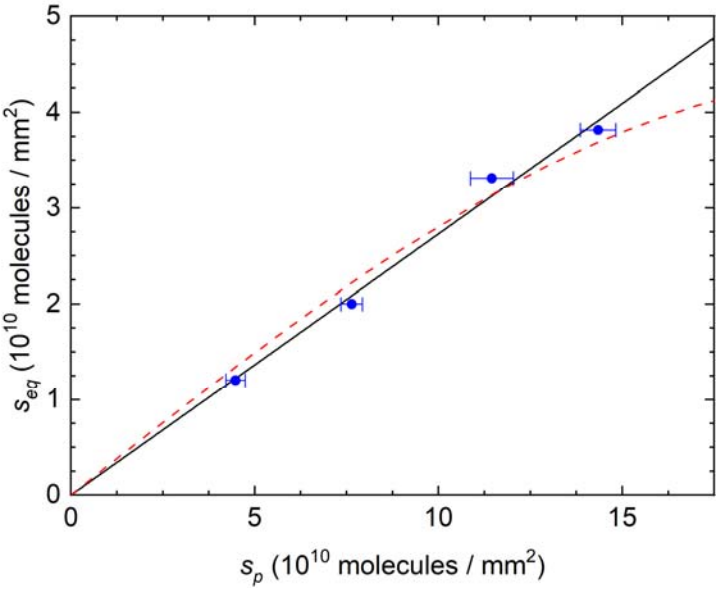

Figure S1. Scaling of hybridization equilibrium amplitude with surface probe density. The blue dots represent the equilibrium amount of DNA target strands measured from spots with different surface density s_p of probes (no linker type). The corresponding binding curves are reported in Figure 2. The black line is a linear fit with slope 0.27. The dashed line is the dependence computed from the numerical solution of Eq. 6 with $\Gamma = 0.9$.

3. Fit of the hybridization kinetic curves with free exponential growth functions

The increase of surface density of targets $\sigma_t(t)$ binding to the immobilized probes can show a non-ideal behaviour at large surface density of probes σ_p. Figure S2 reports $\sigma_t(t)$ measured for probes with no linker (probe p1) after the addition of targets in solution at the concentration c_t of 100 nM. Under the hypothesis of an ideal interaction described by the Langmuir model, we fitted the hybridization curves with simple exponential growth functions without constraints (Eq. 2). As shown in Figure S2, only the binding curve corresponding to the spots with the smallest σ_p was rather well fitted by an exponential growth (blue curves), and the deviation progressively increases with increasing σ_p. This behaviour suggests that the Langmuir interaction model does not represent well the hybridization kinetics between 12mers for large surface densities of probes.

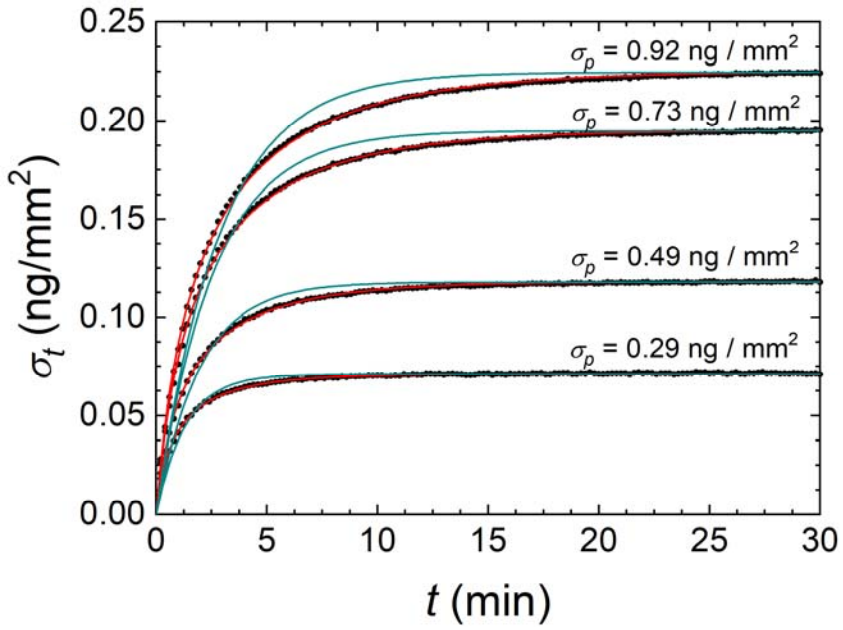

Figure S2. Free exponential fit of the hybridization kinetic curves measured by RPI. The black dots and the red curves are mass surface density data and NLER model fits shown in Figure 2 of the main text, respectively. The binding curves refer to spots on the same RPI sensor with different surface density σ_p of DNA probes (no linker type) and are measured after the injection of 100 nM of target DNA in solution with 150 mM NaCl. The light blue curves represent the best fits with single exponential growth functions without constraint.

4. Increase of electrostatic repulsion with probe surface density

Coherently with previous models describing the equilibrium behaviour of DNA surface hybridization (2)(3), the NLER kinetic model also accounts for an electrostatic repulsion increasing with the surface density of probes. The hybridization process becomes progressively non-Langmuir as the surface density of probes increases. This behaviour is accounted for by the parameter Γ in Eq. 6. If large enough, the value of Γ can be estimated from the dependence of the amplitudes and rates of the hybridization curves with c_t at constant probe density s_p. Figure S3 shows the values of Γ extracted from the fit of the hybridization curves measured for the no linker probe type, which is the case with larger n and hence larger observable deviations from a Langmuir model. The values of Γ are consistent with a liner scaling with s_p, as $\Gamma = \gamma s_p$ (Eq. 7). On the basis of this observation and on the analogous dependence predicted in (3), for each experiment we fitted the amplitudes and rates of the hybridization curves as a function of both c_t and s_p, assuming a linear dependence between Γ and s_p.

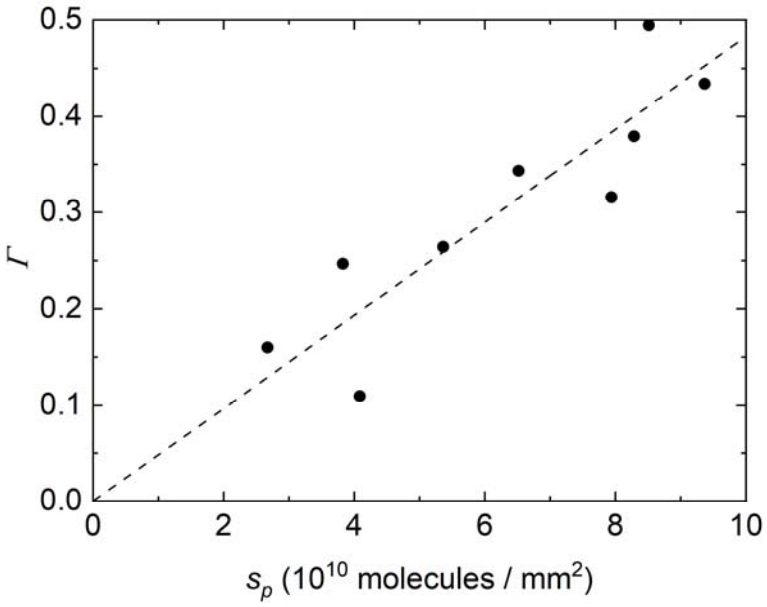

Figure S3. Measured dependence of electrostatic repulsion parameter Γ on the surface density of probes. Values of Γ obtained from the fit of the hybridization curves with the solutions of Eq. 6 for different surface density of probes (no linker type). The line is a linear fit with slope $\gamma = 0.48 \cdot 10^{-10}$ mm^2.

5. Fit quality of equilibrium curves

The equilibrium data reported in Figure 3b of the main text are better fitted by the NLER model then by the Langmuir model. In Table S1, we report the R^2 values and the residual sum of squares values (RSS) for both fits shown in Figure 3b (blue and green lines for the Langmuir and NLER model, respectively). The R^2 values for NLER model are constantly larger than those for the Langmuir model, whereas the RSS are constantly smaller. This means that the NLER model produces fits that represent the data more accurately, as also clear by visual inspection of Figure 3b. Additionally, the fit quality of the Langmuir model decreases with the increase of probe density, indicating that the DNA hybridization equilibrium data deviate more from the Langmuir model at larger probe densities. This observation is coherent with the results reported in this work.

Table S1. R^2 values and residual sum of squares (RSS) for fits to equilibrium curves in Figure 3b.

	Langmuir model		**NLER model**	
σ_p (ng/mm^2)	**R^2**	**RSS**	**R^2**	**RSS**
0.19	0.9904	$6.6 \cdot 10^{-5}$	0.9964	$2.5 \cdot 10^{-5}$
0.24	0.9887	$2.8 \cdot 10^{-4}$	0.9986	$3.3 \cdot 10^{-5}$
0.38	0.9853	$8.1 \cdot 10^{-4}$	0.9989	$6.2 \cdot 10^{-5}$
0.41	0.9836	$1.0 \cdot 10^{-3}$	0.9993	$4.5 \cdot 10^{-5}$

The residual analysis of fits in Figure 3b is shown in Figure S4. Results indicate that the NLER model is both more precise and more accurate than the Langmuir model, as indicated by the vicinity of the red dots to the zero line and their reduced spread. The larger residuals at the lowest target concentrations (c_t = 0.5) is ascribed to a lower accuracy in determining the equilibrium amplitudes of the binding curves. Overall, the difference in the fit quality between the two models increases with probe density, suggesting that the Langmuir model indeed does not represent well DNA hybridization on a surface at large probe densities.

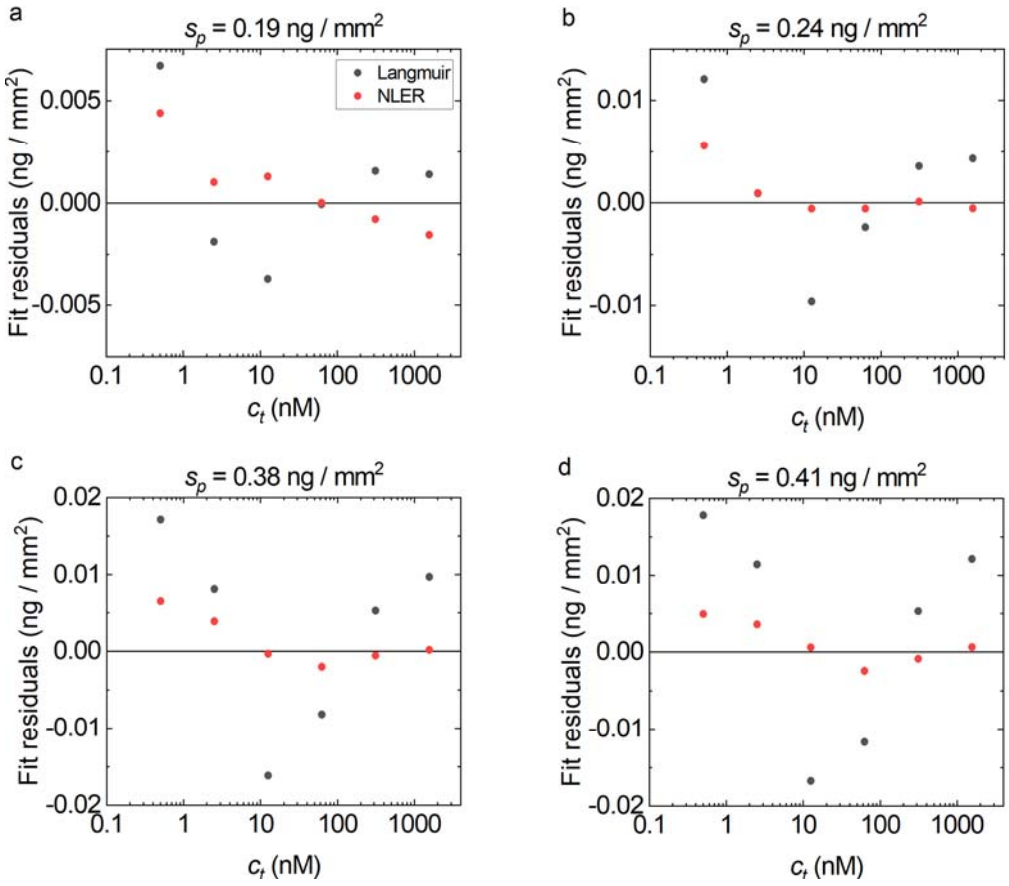

Figure S4. Fit residuals for the equilibrium data of Figure 3b. The residuals are calculated as the difference between observed value and predicted value, from the fits of both Langmuir and NLER model. NLER model fit residuals are shown as red dots, Langmuir model fit residuals are shown as grey dots. NLER model is systematically more accurate than the Langmuir model across all observed target injections, as seen in the distance from the zero line. Smaller deviation of red dots indicate that the NLER model is also more precise than its Langmuir counterpart.

References

1. Salina, M., F. Giavazzi, R. Lanfranco, E. Ceccarello, L. Sola, M. Chiari, B. Chini, R. Cerbino, T. Bellini, and M. Buscaglia. 2015. Multi-spot, label-free immunoassay on reflectionless glass. Biosens. Bioelectron. 74: 539–545.
2. Vainrub, A., and B.M. Pettitt. 2002. Coulomb blockage of hybridization in two-dimensional DNA arrays. Phys. Rev. E. 66: 041905.
3. Halperin, A., A. Buhot, and E.B. Zhulina. 2004. Sensitivity, Specificity, and the Hybridization Isotherms of DNA Chips. Biophys. J. 86: 718–730.